SEMARAK ILMU PUBLISHING

Journal of Advanced Research in Fluid Mechanics and Thermal Sciences

Journal homepage:
https://semarakilmu.com.my/journals/index.php/fluid_mechanics_thermal_sciences/index
ISSN: 2289-7879

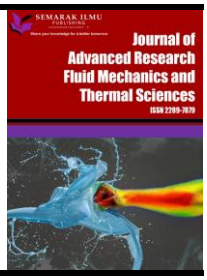

Peristaltic Flow of Jeffrey Fluid in an Inclined Porous Tube with Multi-Thrombosis

Thamatam Vamsidar[1,*], Krishna Kumari Gannamaraju[2], Raja Shehar Mamidi Narsimha[3]

[1] Department of Mathematics, Keshav Memorial Institute of Technology, Hyderabad, India
[2] Department of Mathematics, Aurora Deemed to be University, Hyderabad, India
[3] Department of Mathematics, Jawaharlal Nehru Technological University, Hyderabad, India

ARTICLE INFO

Article history:
Received 20 May 2024
Received in revised form 29 August 2024
Accepted 14 September 2024
Available online 30 September 2024

ABSTRACT

The fact that multiple thrombosis opposes blood flow and flow is rare in blood vessels is refined to a normal condition with catheter application. The inner surface of the circular blood arteries may not be smooth in the majority of diseased instances. Additionally, the small blood vessel peristalsis mechanism is formed. In this paper, we discuss a mathematical model for the flow of biological fluid (blood) in a circular tube with multi-thrombosis considered under peristaltic wave propagation. The blood flow in this tube is restricted due to the many thromboses present, and the flow is redesigned with the aid of a catheter. We model this non-Newtonian blood flow issue for Jeffrey fluid. In most pathological cases, the inner surface of the circular blood vessels may not be smooth. Further, the mechanism of the peristalsis is established for small blood vessels. Because of this biological phenomenon, the peristaltic movement of Jeffrey fluid in a porous annulus with slip is examined. Equations that govern energy and momentum are solved exactly, and graphical interpretation is made using mathematical software. Streamline graphs show the many thromboses that increase in height. The wall shear stress graphs show a sinusoidally advancing wave with peaks and dips of different amplitudes. This tube's unique crest and trough amplitude are caused by the presence of multiple thromboses. We obtained the impact of the pressure gradient on the permeability parameter (β). The pressure gradient falls as the permeability parameter rises.

Keywords:
Peristaltic flow; Jeffrey fluid; inclined porous; multi-thrombosis

1. Introduction

Peristalsis is the term for the phenomena that describes how biological fluid moves inside a tube with walls that move in a sinusoidal pattern. Transportation generated by peristaltic motion is characterized by the slow growth and expansion of the constricted space along the tube wall. Peristalsis is crucial for the movement of nutrients from the oropharynx into the bladder, urine from the kidneys, blood from the heart, and many fluids such as bile in the bladder. Peristaltic mechanisms in physiological systems have become popular due to the understanding of numerous biological flows. Vaidya *et al.,* [1] analyzed Jeffrey nanofluidic mass or heat transfer in vertical channels during

* *Corresponding author.*
E-mail address: vamshidhar.thamatam@gmail.com

https://doi.org/10.37934/arfmts.121.2.174191

MHD peristalsis. Mopuri *et al.,* [2] studied a viscous, incompressible, electrically conducting, non-Newtonian Jeffery fluid in an unstable, MHD natural convective boundary layer flow across a semi-infinite vertically inclined permeable moving plate immersed in a porous material. Nadeem *et al.,* [3] studied heated Jeffrey fluid with peristaltic flow within a channel, including an elliptical cross section. Gudekote and Choudhari [4] have been investigated the effect of inclination and slide on the Casson fluid's peristaltic movement in an elastic tube with porous walls. Hamrelaine *et al.,* [5] was mathematically explained that the magnetohydrodynamic flow between two solid porous plates meeting at an angle or through non-parallel porous walls can be thought of as a combination of one injection/suction and the classical Jeffrey Hamel flow. Manjunatha *et al.,* [6] investigated a Jeffrey fluid flowing peristaltically through a non-uniform channel with varying viscosity and thermal conductivity while experiencing heat and mass transfer effects. Madhukesh *et al.,* [7] examined the non-Newtonian (micropolar-Casson) steady-state incompressible flow of fluids trapped between two parallel porous disks. Rajashekar *et al.,* [8] investigated on the impact of variations in mass and temperature on the peristaltic flow of Rabinowitsch fluid via irregular channels. Madhukesh *et al.,* [9] investigated the effects of a Casson-Maxwell non-Newtonian nanofluid, magnetized and incompressible, between two stationary porous disks.

Jeffrey fluid is a non-Newtonian fluid model that has attracted the attention of many researchers due to its ability to represent fluid in the body. It turns out that one of the fundamental models that most effectively refines the best description of the characteristics of a viscoelastic fluid is Jeffrey's fluid flow model. Bajwa *et al.,* [10] In an infinite horizontal porous plate, we investigated how porosity and MHD affect the fluid's velocity. Channakote *et al.,* [11] studied the theoretical propagation of Jeffrey fluid's peristaltic waves in a non-uniform tube under the influence of convective boundary conditions and viscous dissipation. Krishna *et al.,* [12] covered Hall current and electric current result when a magnetic field perpendicular to the channel affects access to Jeffrey's MHD flow through porous media in vertical stages. Ramesh *et al.,* [13] investigated EMHD liquid flow on a surface with microstructural slippage. Energy and mass profiles have taken into account the impacts of a uniform heat source/sink (HS/S) with homogeneous and heterogeneous chemical processes. Rani *et al.,* [14] examined MHD natural convective boundary layer flow across a semi-infinite vertically inclined permeable moving plate immersed in a viscous, non-Newtonian Jeffrey fluid porous medium that is incompressible, conducting, and porous. Nallapu and Radhakrishnamacharya [15] A two-fluid model of the flow of Jeffrey liquid in a narrow tube in the presence of a magnetic field was examined. Kumar *et al.,* [16] Peristaltic applications of Jeffrey fluids in asymmetric channels with long-wavelength permeable walls and low Reynolds conditions are discussed.

Kodi and Mopuri [17] studied the effects of Soret-aligned magnetic fields and chemical reactions during the flow of unstable MHD oscillating Carson fluid through inclined vertical porous plates. Vijayaragavan *et al.,* [18] examined the existence of the reaction and the Dufour effect on heat and mass conversion in MHD Casson fluid flow through an inclined porous plate. Ahmed *et al.,* [19] examined the existence of the reaction and the Dufour effect on heat and mass conversion in MHD Casson fluid flow through an inclined porous plate. Manchi and Ponalagusamy [20] theoretically investigated inclined porous narrowed arterial stenosis under the simultaneous influence of electroosmotic on pulsatile Sutter nanofluid flow. Sandhya *et al.,* [21] heat, radiation, chemical reactions, and MHD flow around a porous plate for mass and heat transfer are analyzed. Manjunatha *et al.,* [22] examined the effects of water flow on heat transfer and viscosity change while the Casson fluid passed through an inclined, porous, axisymmetric tube. Krishna *et al.,* [23] investigated the effects of cilia, a porous media, a magnetic field, and channel tilt on the micropolar fluid under various boundary conditions. Sharma and Yadav [24] examined a two-layered mathematical model of non-Newtonian blood flow via porous constricted blood arteries. The core zone of blood flow contains

the non-Newtonian Casson fluid, or suspension of erythrocytes, whereas the periphery region contains the Newtonian fluid, or plasma flow.

The development of a thrombus inside the artery restricts the flow of blood to the body's major organs. It forms as a result of fats, cholesterol, and other substances building up. Using a catheter helps the blood flow through these damaged arteries. When placed into such damaged arteries, this hollow, thin, fine tube eventually improves flow. Saleem *et al.,* [25] mathematical description of thrombus in cannulated blood vessels using microphysical analysis of peristaltic flow in carbon nanotubes, SWCNTs, and MWCNTs. Abuiyada *et al.,* [26] examined how the MHD peristaltic flow of Jeffrey nanofluids in an inclined symmetric channel through a porous medium is affected by the chemical reaction and activation energy. Saleem *et al.,* [27] blood clots in the area, blood flow through catheterized vessels, and small walls are checked. Akthar *et al.,* [28] investigated mathematically using a catheter to pass blood through multiple thromboses inside a tube. Misra *et al.,* [29] explained why blood flow in intraductal stenotic arteries behaves in a non-Newtonian manner. Shahzadi and Nadeem [30] the peristaltic flow of nanofluid in the ring region of an inclined ring was investigated in relation to the effects of a gradient magnetic field and copper nanoparticles. Reddy *et al.,* [31] a mathematical analysis has been conducted on blood flow through constricted blood arteries when a catheter is in place. Sharma *et al.,* [32] examined the two-layered, narrow tube Jeffrey-fluid model with mild stenosis. The blood flow in small arteries is represented as a two-fluid system using erythrocyte suspension.

All the physiological tubes are not horizontal; in abnormal cases, the tube walls may not be smooth. Hence, the inclination of the tube, together with wall slip, is important in the flow investigation. We have applied transformation to make the unsteady problem a steady one. In the present work, we want to examine the effects of catheterization on the blood flow of biological fluids in a circular tube with multi-thrombosis considered under peristaltic wave propagation. In most pathological cases, the inner surface of the circular blood vessel may not be smooth; the slip parameter is considered and mathematically investigated. One of the notable pumping characteristics is Δp or $\frac{dp}{dx}$. I therefore had conversations about temperature, velocity, and pressure gradient. The problem's exact solutions are computed. Using Mathematica software, streamlines are plotted, and the results are presented graphically.

2. Mathematical Model

A mathematical investigation is conducted on the peristaltic blood flow within a geometry that exhibits multi-thrombosis. The blood flow via the tube is decreased by the numerous clots present, and a catheter (Figure 1) is used to restore the blood flow.

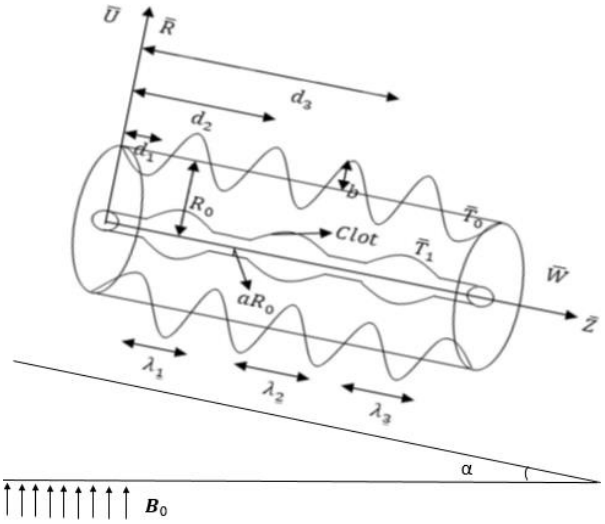

Fig. 1. Geometry of the problem

The dimensional mathematical equations for the tube's inner surface $\overline{\in}\ (z)$, which has numerous clots, and outer surface $\overline{\eta}(z)$, which has a moving sinusoidal wave, are given [28]

$$\overline{\eta}(z) = R_0 + b\,Sin\left(\frac{2\pi}{\lambda}\left(\overline{Z} - c\overline{t}\right)\right) \tag{1}$$

$$\overline{\in}\ (z) = \begin{cases} R_0[a + f_1(\bar{z})], d_l \le z \le d_l + \lambda_1 \\ R_0 a \qquad\qquad otherwise \end{cases}, \tag{2}$$

Here, $f_1(\bar{z})$ describes the geometry of the poly-thrombosis. The governing equations of the flow become are

$$\frac{\partial \overline{U}}{\partial \overline{R}} + \frac{\overline{U}}{\overline{R}} + \frac{\partial \overline{W}}{\partial \overline{Z}} = 0, \tag{3}$$

$$\rho\left(\frac{\partial \overline{U}}{\partial \overline{t}} + \overline{U}\frac{\partial \overline{U}}{\partial \overline{R}} + \overline{W}\frac{\partial \overline{U}}{\partial \overline{Z}}\right) = -\frac{\partial \overline{P}}{\partial \overline{R}} + \frac{1}{\overline{R}}\frac{\partial}{\partial \overline{R}}\left(\overline{RS}_{\overline{RR}}\right) + \frac{\partial}{\partial \overline{Z}}\left(\overline{S}_{\overline{RZ}}\right) + \rho\bar{f}_R \tag{4}$$

body force $\bar{F} = \left(\bar{f}_R, 0, \bar{f}_Z\right)$

$$\rho\left(\frac{\partial \overline{W}}{\partial \overline{t}} + \overline{U}\frac{\partial \overline{W}}{\partial \overline{R}} + \overline{W}\frac{\partial \overline{W}}{\partial \overline{Z}}\right) = -\frac{\partial \overline{P}}{\partial \overline{Z}} + \frac{1}{\overline{R}}\frac{\partial}{\partial \overline{R}}\left(\overline{RS}_{\overline{RZ}}\right) + \frac{\partial}{\partial \overline{Z}}\left(\overline{S}_{\overline{ZZ}}\right) + \rho\bar{f}_Z \tag{5}$$

$$\rho C_P\left(\frac{\partial \overline{T}}{\partial \overline{t}} + \overline{U}\frac{\partial \overline{T}}{\partial \overline{R}} + \overline{W}\frac{\partial \overline{T}}{\partial \overline{Z}}\right) = \overline{S}_{\overline{RR}}\frac{\partial \overline{U}}{\partial \overline{R}} + \overline{S}_{\overline{RZ}}\frac{\partial \overline{W}}{\partial \overline{R}} + \overline{S}_{\overline{ZR}}\frac{\partial \overline{U}}{\partial \overline{Z}} + \overline{S}_{\overline{ZZ}}\frac{\partial \overline{W}}{\partial \overline{Z}} + k\left(\frac{\partial^2 \overline{T}}{\partial \overline{R}^2} + \frac{1}{\overline{R}}\frac{\partial \overline{T}}{\partial \overline{R}} + \frac{\partial^2 \overline{T}}{\partial \overline{Z}^2}\right) \tag{6}$$

Jeffrey fluid tensor of additional stress determined

$$\overline{S} = \frac{\mu}{1+\lambda_1}(\dot{\gamma} + \lambda_2\ddot{\gamma}) \tag{7}$$

The relationship between fixed coordination and joint movement is as follows

$$\overline{r} = \overline{R}, \overline{z} = \overline{Z} - c\overline{t}, \overline{u} = \overline{U}, \overline{w} = \overline{W} - c, \overline{p}(\overline{z}, \overline{r}) = \overline{P}\left(\overline{Z}, \overline{R}, \overline{t}\right) \tag{8}$$

The dimensionless variables used are as follows

$$r=\frac{\overline{r}}{R_0}, z=\frac{\overline{z}}{\lambda}, u=\frac{\lambda\overline{u}}{R_0 c}, w=\frac{\overline{w}}{c}, t=\frac{c\overline{t}}{\lambda}, p=\frac{R_0^2\overline{p}}{c\lambda\mu_f}, \theta=\frac{\overline{T}-\overline{T}_0}{\overline{T}_1-\overline{T}_0}, \delta=\frac{R_0}{\lambda} \tag{9}$$

where

$$S_{RR}=\frac{2\delta}{1+\lambda_1}\left[1+\frac{\lambda_2 c\delta}{R_0}\left(u\frac{\partial}{\partial r}+w\frac{\partial}{\partial z}\right)\right]\frac{\partial u}{\partial r},$$

$$S_{RZ}=\frac{1}{1+\lambda_1}\left[1+\frac{\lambda_2 c\delta}{R_0}\left(u\frac{\partial}{\partial r}+w\frac{\partial}{\partial z}\right)\right]\left[\frac{\partial w}{\partial r}+\delta^2\frac{\partial u}{\partial z}\right],$$

$$S_{ZZ}=\frac{2\delta}{1+\lambda_1}\left[1+\frac{\lambda_2 c\delta}{R_0}\left(u\frac{\partial}{\partial r}+w\frac{\partial}{\partial z}\right)\right]\frac{\partial w}{\partial z}.$$

Using the long wavelength approximation and low Reynolds number assumption from Eq. (4) to Eq. (6) become

$$\frac{dp}{dz}=\frac{1}{1+\lambda_1}\left[\frac{\partial^2 w}{\partial r^2}+\frac{1}{r}\frac{\partial w}{\partial r}\right]+G\,Sin\,\alpha \tag{10}$$

$$\frac{\partial^2\theta}{\partial r^2}+\frac{1}{r}\frac{\partial\theta}{\partial r}+\frac{B_r}{1+\lambda_1}\left[\frac{\partial w}{\partial r}\right]^2=0 \tag{11}$$

Boundary conditions

$$w+\beta\frac{\partial w}{\partial r}=-1 \;\; at\; r=\eta(z)$$

$$w=-1 \;\; at\; r=\epsilon(z)$$

$$\frac{\partial\theta}{\partial r}=0 \quad at\; r=\epsilon(z) \text{ and } \theta=0 \;\; at\; r=\eta(z). \tag{12}$$

Where $\beta=\frac{\sqrt{Da}}{k}$.

The outside surface $\eta(z)$ as well as the inside surface $\in(z)$ provided are their mathematical expressions without dimensions. The term that is selected for $f_1(\overline{z})$ is

$$\eta(z)=1+\phi\,Sin(2\pi z), \tag{13}$$

$$\overline{\in}(z)=\begin{cases} a+\sigma_1 e^{-\pi^2\left(z-z_{d_1}-0.5\right)^2}, & h_l\le z\le h_l+1, \\ a & otherwise \end{cases} \tag{14}$$

3. Exact Solution

From Eq. (10) we have

$$r^2\frac{\partial^2 w}{\partial r^2}+r\frac{\partial w}{\partial r}=r^2\left(\frac{dp}{dz}-G\,Sin\alpha\right)(1+\lambda_1) \tag{15}$$

Substituting $r = e^z$, $A = \left(\frac{dp}{dz} - G\ Sin\alpha\right)(1 + \lambda_1)$ Eq. (15) is reduced to

$$\frac{\partial^2 w}{\partial z^2} = Ae^{2z} \tag{16}$$

On solving Eq. (16) with the Eq. (12), we have the velocity profile

$$w(r, z) = c_1 + c_2 \log r + \frac{1}{4}\ A\ r^2 \tag{17}$$

where

$$c_1 = -1 - \frac{A}{4}\epsilon^2 - \left[\frac{\log(\epsilon)}{\left[\frac{\beta}{\eta} + \log(\eta) - \log(\epsilon)\right]}\right]\left[\frac{-A}{4}(\eta^2 - \epsilon^2) - \frac{\beta}{2}A\eta\right]$$

$$c_2 = \left[\frac{1}{\left[\frac{\beta}{\eta} + \log(\eta) - \log(\epsilon)\right]}\right]\left[\frac{-A}{4}(\eta^2 - \epsilon^2) - \frac{\beta}{2}A\eta\right]$$

and $A = \left(\frac{dp}{dz} - G\ Sin\alpha\right)(1 + \lambda_1)$

Volumetric flow rate between these two walls

$$\begin{aligned} Q &= 2\pi \int_{\epsilon}^{\eta} r\ w\ dr \\ &= 2\pi\left\{\frac{c_1}{2}(\eta^2 - \epsilon^2) + c_2\left[\log\eta\ \frac{\eta^2}{2} - \log\epsilon\ \frac{\epsilon^2}{2}\right] - \frac{c_2}{4}(\eta^2 - \epsilon^2) + \frac{A}{16}(\eta^4 - \epsilon^4)\right\} \end{aligned} \tag{18}$$

Using the volumetric flow rate we obtain the pressure gradient

$$\frac{dp}{dx} = \frac{\left[\left(\frac{Q}{2\pi}\right) + P_1 P_2 - 2\left(\frac{D}{E}\right)\right]}{(1+\lambda_1)\left[P_3 - P_1\left(\frac{\epsilon^2}{4} - P_4\left(\frac{\log\epsilon}{E}\right) - \left(\frac{\beta\eta}{2}\right)\right) - \left(\frac{D}{E}\right)\left(P_4 - \left(\frac{\beta\eta}{2}\right)\right)\right]} \tag{19}$$

$$D = \left[\frac{log\,\eta}{2}\eta^2 - \frac{log\in}{2}\in^2 - \frac{1}{4}(\eta^2 - \in^2)\right]$$

$$E = \left[\frac{\beta}{\eta} + log\,\eta - log\ \in\right];\ P_1 = \frac{1}{2}(\eta^2 - \in^2);\ P_2 = 1 + 2\left(\frac{log\in}{E}\right);$$

$$P_3 = \frac{1}{16}(\eta^4 - \in^4);\ P_4 = \frac{1}{4}(\eta^2 - \in^2)$$

τ_w is computed as follows

$$\tau_w = -\left.\frac{\partial w}{\partial r}\right|_{r=\eta}$$

From Eq. (11) we have

$$r^2\frac{\partial^2\theta}{\partial r^2}+r\frac{\partial\theta}{\partial r}=-\frac{B_r}{(1+\lambda_1)}{c_2}^2-\frac{B_r}{(1+\lambda_1)}\frac{A^2}{4}r^4-\frac{B_r}{(1+\lambda_1)}c_2Ar^2 \tag{20}$$

on solving Eq. (20) with the Eq. (12), we have the temperature is

$$\theta=c_3+c_4\log r-\frac{B_r}{(1+\lambda_1)}\left[\frac{{c_2}^2}{2}(\log r)^2+\frac{A}{64}(\log r)^4+\frac{c_2A}{4}(\log r)^2\right] \tag{21}$$

where $c_3=c_4(-\log\eta)+\left[\frac{B_r}{(1+\lambda_1)}\right]\left\{\frac{{c_2}^2}{2}(\log\epsilon)^2+\frac{A^2}{16}(\log\epsilon)^4+\frac{c_2A}{4}(\log\eta)^2\right\}$

$$c_4=\frac{B_r}{(1+\lambda_1)}\left\{{c_2}^2\log\epsilon+\frac{A^2}{16}(\log\epsilon)^3+\frac{c_2A}{2}\log\epsilon\right\}$$

4. Results and Discussion

The current study focuses on how catheterization affects biological fluid blood flow in a circular tube with many thromboses when peristaltic wave propagation is taken into consideration. With regard to the impacts of slip and tilt in the tube, the current model is an extension of the research done by Akhtar *et al.,* [28]. One of the notable pumping characteristics is Δp or $\frac{dp}{dx}$. Therefore, I had discussions on pressure gradient, velocity and temperature. Velocity models are drawn and shown in Figure 2, Figure 3, Figure 4 and Figure 5. Figure 2 shows the effect of amplitude (ϕ) on velocity profile. Although the velocity distribution is more positive in the region close to the region between two walls, the velocity distribution shows a lower behavior towards depth as the value ϕ increases. The development of peristaltic transport occurs due to the increase in the amplitude of the peristaltic wall. The velocity profile increases near the central region.

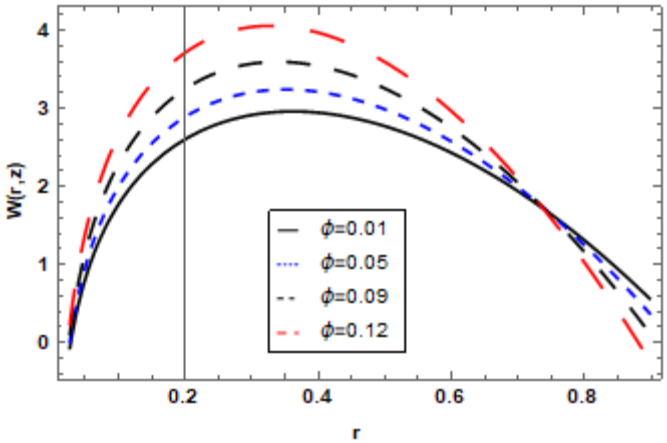

Fig. 2. Velocity profile using $\emptyset$ for $\lambda_1=0.5,\alpha=\frac{\pi}{3},\ d_a=0.01,G=0.5,Z=0.3,Zd=0.5,h_1=0.5,a=0.1,Q=0.1,\sigma_1=0.01$

Figure 3 shows that as the value of Q increases, there will be an increase in the velocity profile near the central region. In Figure 4, it turns out the velocity rise with a poly – thrombus wall, but decreases with increasing σ1 value of peristaltic walls.

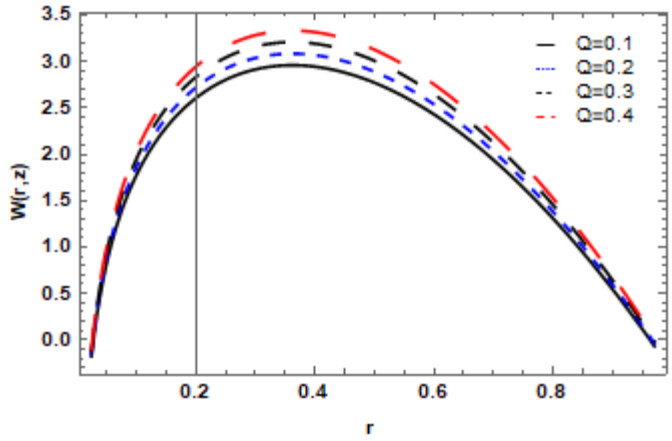

Fig. 3. Velocity profile using Q for $\lambda_1 = 0.5, \alpha = \frac{\pi}{3}, d_a = 0.01, G = 0.5, Z = 0.3, Zd = 0.5, h_1 = 0.5, a = 0.1, \phi = 0.1, \sigma_1 = 0.01$

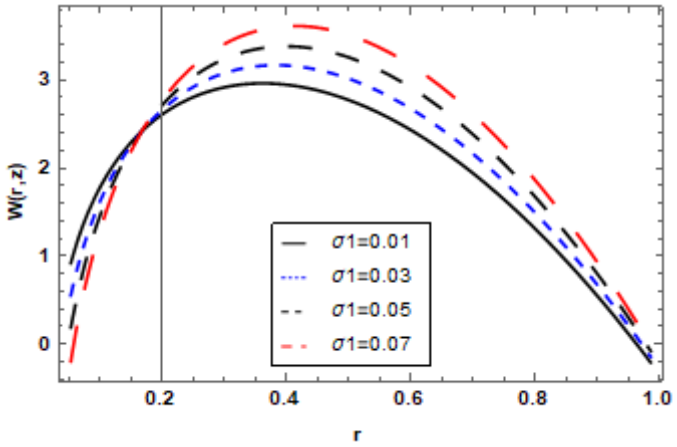

Fig. 4. Velocity profile for $\lambda_1 = 0.5, \alpha = \frac{\pi}{3}, d_a = 0.01, G = 0.5, Z = 0.3, Zd = 0.5, h_1 = 0.5, a = 0.1, Q = 0.1, \phi = 0.1$

Figure 5 interprets the impact of permeability parameter (β) on velocity profile. The velocity distribution obtains the majority of higher values closer to the central region. There is a decrement in the permeability parameter.

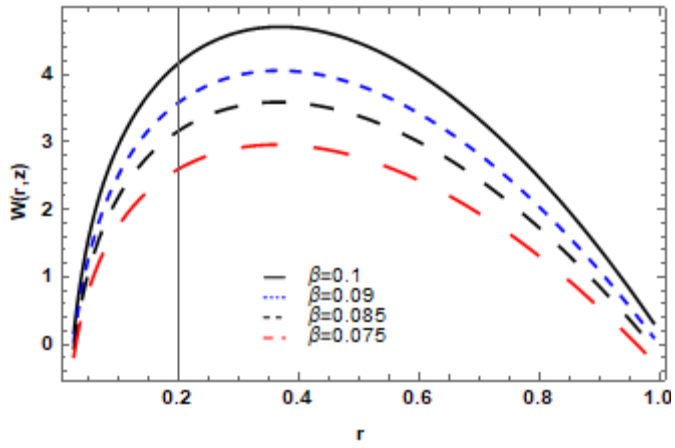

Fig. 5. Velocity profile using permeability parameter for $\lambda_1 = 0.5, \alpha = \frac{\pi}{3}, G = 0.5, Z = 0.3, Zd = 0.5,\ h_1 = 0.5, a = 0.1, Q = 0.1, \phi = 0.1, \sigma_1 = 0.01$

Figure 6 and Figure 7 have a discussion about shear stress τ_w plotted against axial coordinates. From Figure 6, it was found that as the Q value increases, the shear stress value decreases. In this figure, it can be seen that the sine wave shows peaks and valleys at different amplitudes. The presence of many thrombi in this tube is the reason why the peak and trough amplitudes are clearly different. In Figure 7 it shows that as the value of σ1 increases, the value of the increase is exactly where multi – thrombosis occurs.

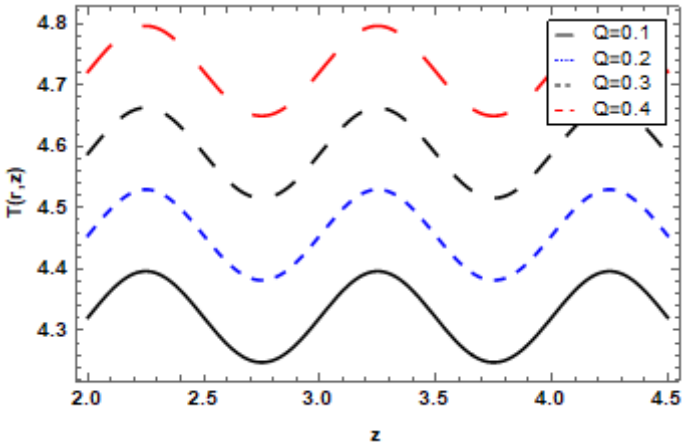

Fig. 6. Shear stress τ_w for $\lambda_1 = 0.5, \alpha = \frac{\pi}{3}, d_a = 0.01, G = 0.9, Z = 0.3, Zd = 0.5, h_1 = 0.5, a = 0.1, \sigma_1 = 0.1, \phi = 0.05$

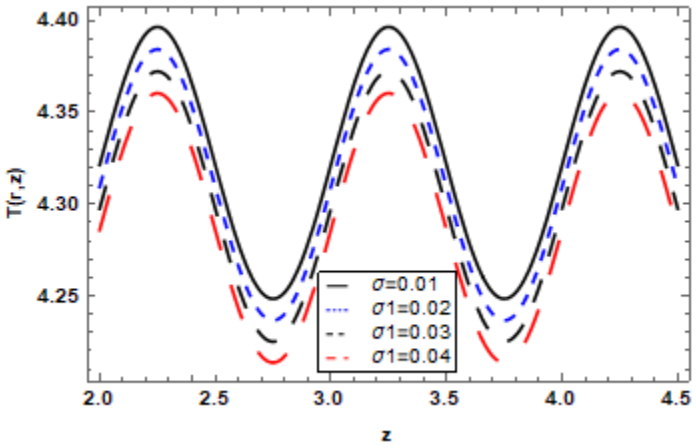

Fig. 7. Shear stress τ_w for $\lambda_1 = 0.5, \alpha = \frac{\pi}{3}, d_a = 0.01, G = 0.9, Z = 0.3, Zd = 0.5, h_1 = 0.5, a = 0.1, Q = 0.1, \phi = 0.05$

The temperature profile graphically discussed for different parameters in Figure 8, Figure 9, Figure 10, Figure 11 and Figure 12. From Figure 8, it can be seen that as the Br value increases, the temperature distribution also increases, and viscous dissipation rather than molecular material is the main reason for electricity generation. Figure 9 reveals that there is a decline in temperature profile for increasing values of $\lambda 1$. In Figure 10, the temperature represents the end of various thrombi, and it is more beneficial to increase the value of ϕ. In Figure 11, it is observed that, due to increment in Q, temperature attains an increase. Figure 12 show that the temperature curve decreases as the value of σ1 increases.

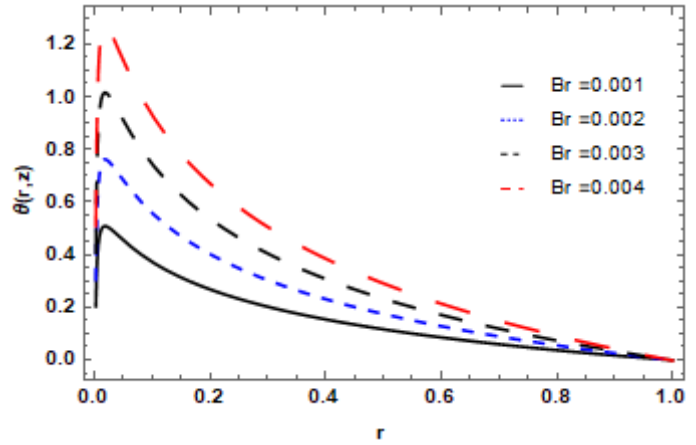

Fig. 8. Variability of temperature profile for $\lambda_1 = 0.5, \alpha = \frac{\pi}{6}, d_a = 0.1, k = 0.8, G = 0.5, Z = 0.9, Zd = 0.5, h_1 = 0.5, a = 0.01, Q = 0.2, \phi = 0.3, \sigma_1 = 0.01$

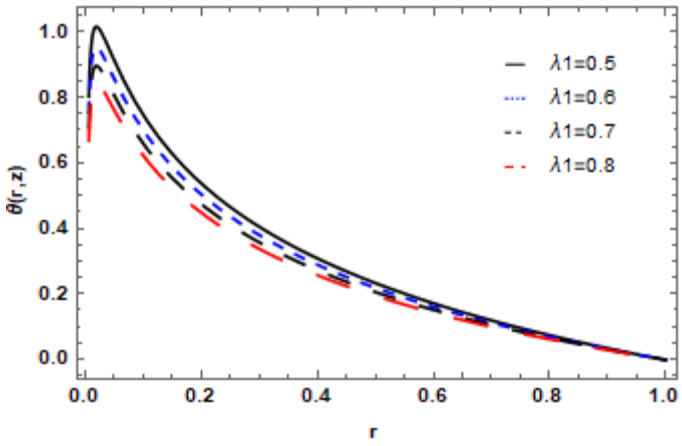

Fig. 9. Variability of temperature profile for $B_r = 0.002, \alpha = \frac{\pi}{6}, d_a = 0.1, k = 0.8, G = 0.5, Z = 0.9,\ Zd = 0.5, h_1 = 0.5, a = 0.01, Q = 0.2, \phi = 0.3, \sigma_1 = 0.01$

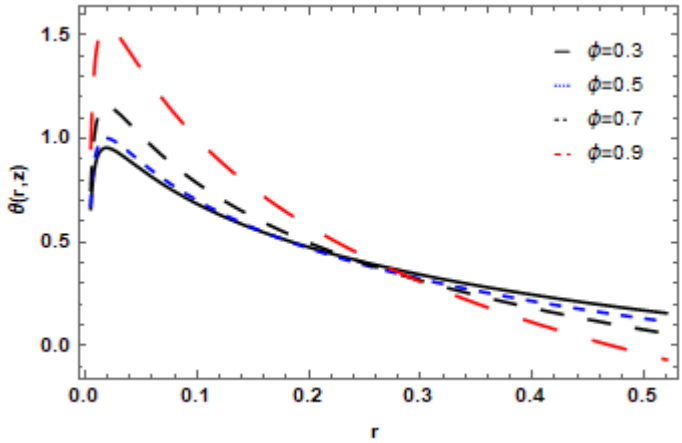

Fig. 10. Variability of temperature profile for $\lambda_1 = 0.5, \alpha = \frac{\pi}{6}, d_a = 0.1, k = 0.8, G = 0.5, Z = 0.9,\quad Zd = 0.5, h_1 = 0.5, a = 0.01, Q = 0.2, B_r = 0.002, \sigma_1 = 0.01$

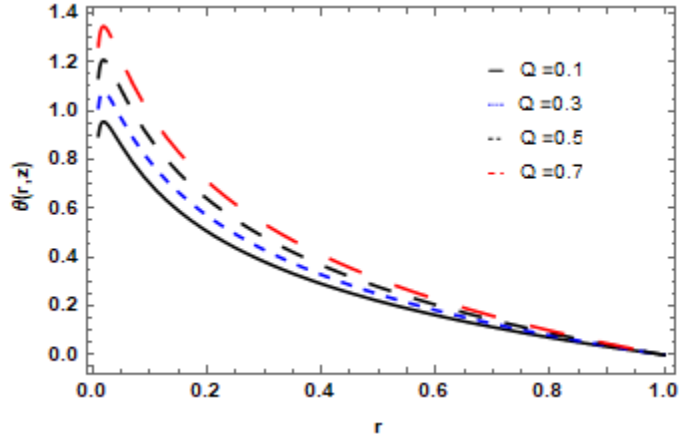

Fig. 11. Variability of temperature profile for $\lambda_1 = 0.5, \alpha = \frac{\pi}{6}, d_a = 0.1, k = 0.8, G = 0.5, Z = 0.9,\quad Zd = 0.5, h_1 = 0.5, a = 0.01, \phi = 0.3, B_r = 0.002, \sigma_1 = 0.01$

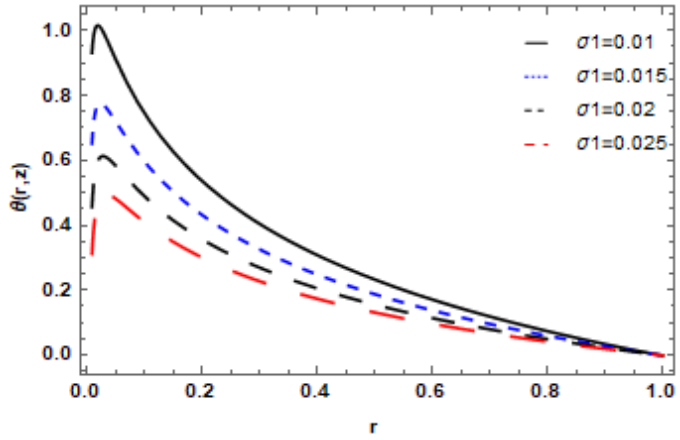

Fig. 12. Variability of temperature profile for $\lambda_1 = 0.5, \alpha = \frac{\pi}{6}, d_a = 0.1, k = 0.8, G = 0.5, Z = 0.9, \quad Zd = 0.5, h_1 = 0.5, a = 0.01, \phi = 0.3, B_r = 0.002$

Figure 13 explain the effect of the permeability parameter (β) on the pressure gradient. As the permeability parameter increases, the pressure gradient decreases.

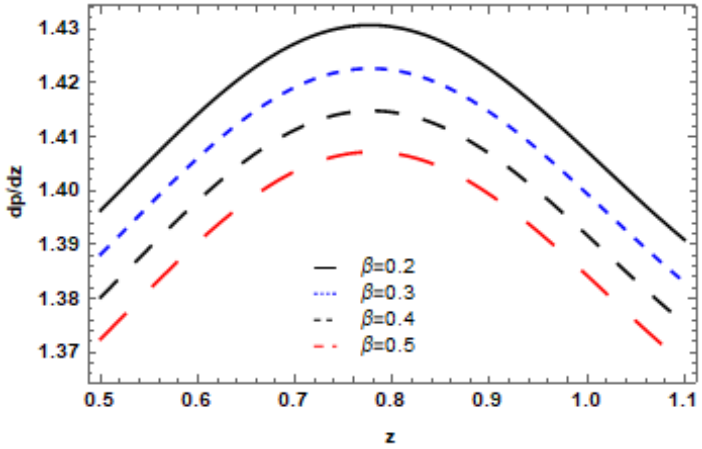

Fig. 13. Variability of pressure gradient for $\lambda_1 = 0.5, \alpha = \frac{\pi}{6}, G = 0.5, Zd = 0.5, h_1 = 0.5, a = 0.01, \phi = 0.03, B_r = 0.002, \sigma_1 = 0.01$

Plots of streamlines are made for various flow rate Q values, as given in Figure 14 and Figure 15 for fixed height of multi – thrombosis. It is clear from the streamlines that as Q increases, the size of the trapping decreases but the number increases. In this case, a sine wave is seen at one end, and multiple thrombi are seen at the other end. Draw an assembly line for various thrombi at different heights (Figure 16, Figure 17 and Figure 18), and changes in these graphs were noted. Figure 16, Figure 17, and Figure 18 show that as the σ1 value increases, the height of multi-thrombosis also increases.

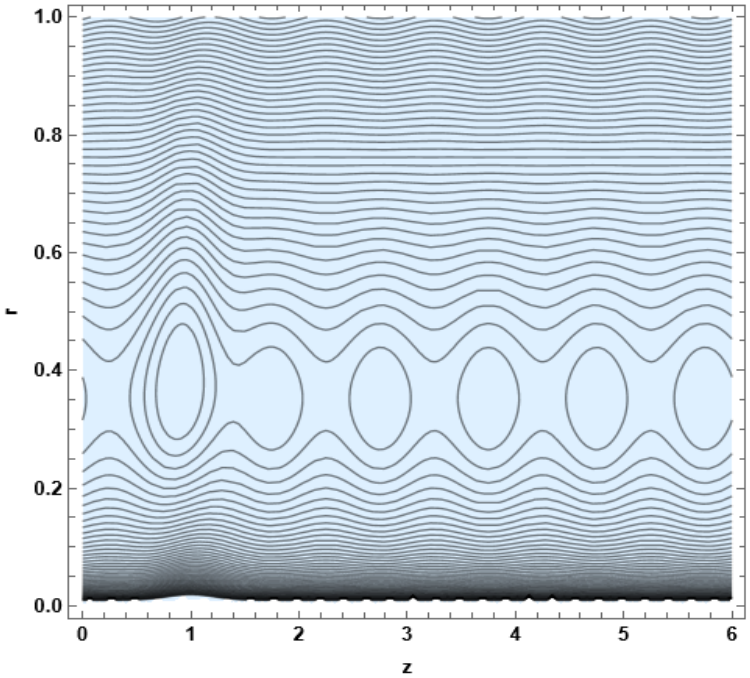

Fig. 14. Streamlines for $Q = 0.4$ with $\lambda 1 = 0.5; G = 0.5; k = 0.9; \mathrm{da} = 0.005;\ \phi = 0.01; \mathrm{zd} = 0.5; \mathrm{h1} = 0.5; a = 0.01; \sigma 1 = 0.01; \alpha = \pi/6$

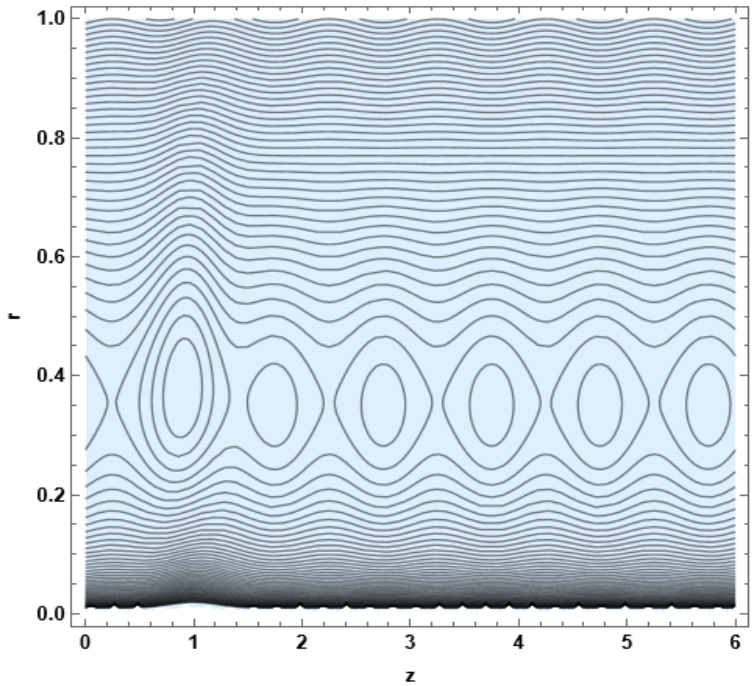

Fig. 15. Streamlines for $Q = 0.5$ with $\lambda 1 = 0.5; G = 0.5; k = 0.9; \mathrm{da} = 0.005;\ \phi = 0.01; \mathrm{zd} = 0.5; \mathrm{h1} = 0.5; a = 0.01; \sigma 1 = 0.01; \alpha = \pi/6$

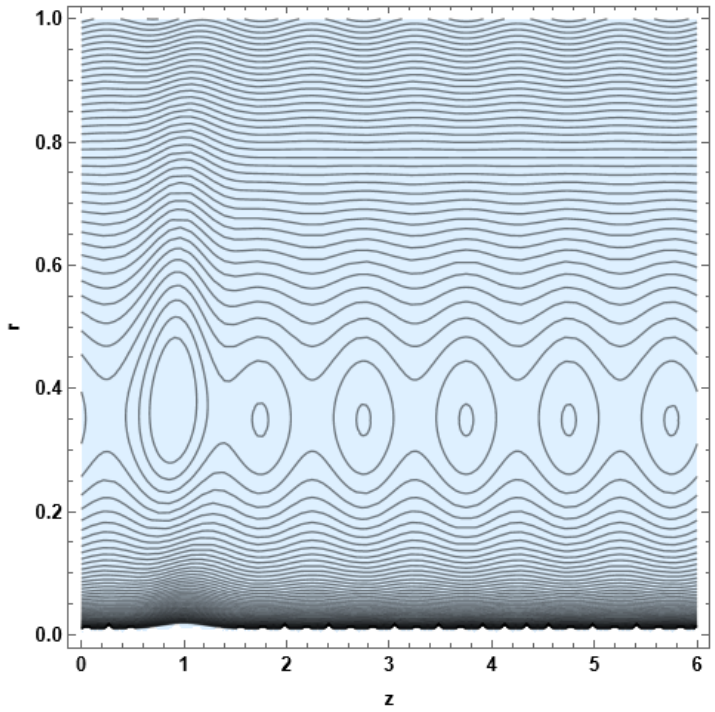

Fig. 16. Streamlines for $\sigma 1 = 0.01$ with $\lambda 1 = 0.5; G = 0.5;\ k = 0.5; \mathrm{da} = 0.01;\ \phi = 0.01; \mathrm{zd} = 0.5; \mathrm{h1} = 0.5; a = 0.1; Q = 0.3; \alpha = \pi/6$

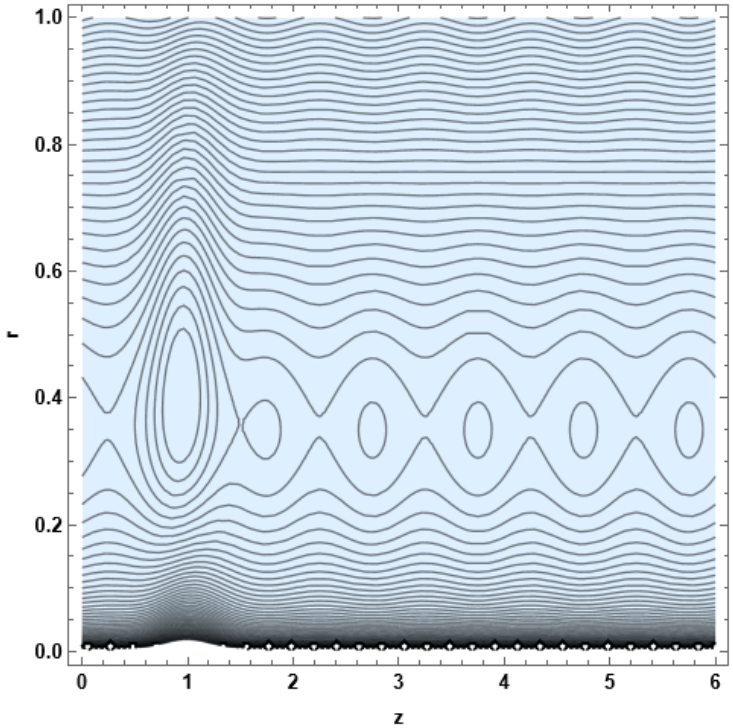

Fig. 17. Streamlines for $\sigma 1 = 0.02$ with $\lambda 1 = 0.5; G = 0.5; k = 0.5; \mathrm{da} = 0.01;\ \phi = 0.01; \mathrm{zd} = 0.5; \mathrm{h1} = 0.5; a = 0.1; Q = 0.1; \sigma 1 = 0.04; \alpha = \pi/6$

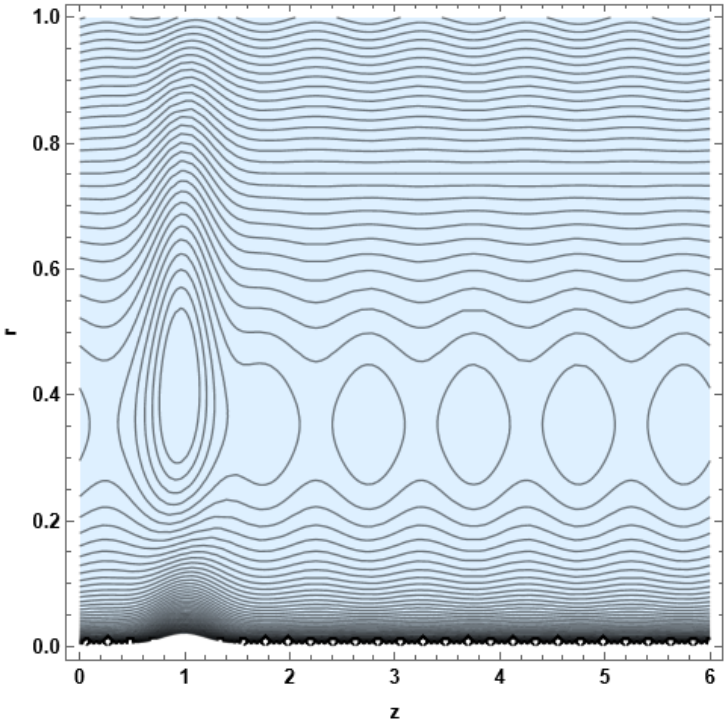

Fig. 18. Streamlines for $\sigma 1 = 0.025$ with $\lambda 1 = 0.5; G = 0.5; k = 0.5; \mathrm{da} = 0.01;\ \phi = 0.01; \mathrm{zd} = 0.5; \mathrm{h1} = 0.5; a = 0.1; Q = 0.1; \sigma 1 = 0.04; \alpha = \pi/6$

Figure 19 compares the results of the present and Akhtar *et al.,* [28] models for a fixed maximum thrombus height (σ1). The results of the present model are plotted by taking *Da* = 0 and α = 0 to show the comparison with their model. It is clear from Figure 19 that the results of the present model exactly match their results, which also validate our results.

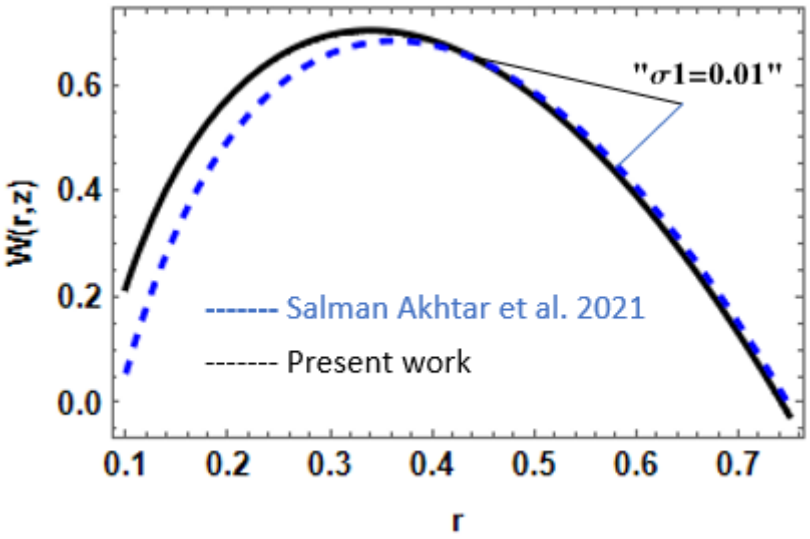

Fig. 19. Results for a fixed maximum thrombus height (σ1) present vs Akhtar *et al.,* [28]

5. Conclusions

Peristalsis of multi thrombosis with Jeffrey fluid in a tube has been studied mathematically. The presence of these vessels reduces blood flow in the vessels, and a catheter is placed to restore blood flow. The main results of this mathematical research are described below.

i. The velocity distribution almost increases in amplitude near the central area of both walls, but exhibits a lower characteristic with increasing ϕ (ratio of amplitude to mean radius) near the peristaltic surface.
ii. The velocity distribution decreases as the thrombus wall increases, but remains constant as the $\sigma 1$ value increases in the peristaltic wall.
iii. For reduced permeability parameter values, the size of the velocity profile increases almost around the area between the two walls.
iv. The sinusoidal traveling wave shown in the wall stress map has peaks and troughs of different amplitudes. The presence of various thrombi in these vessels is responsible for the difference between height and trough amplitudes.
v. Protrusions with high amplitude show the place where there are many thrombi, while protrusions with low amplitude show the place where there is no thrombus.
vi. The axial pressure gradient $\left(\frac{dp}{dx}\right)$ with increased amplitude is almost at the center of the walls for decreasing values of permeability parameter.
vii. The sine wave is clearly visible at one end of the streamline diagram, and numerous thrombi are visible at the other end.

Acknowledgement
This research was not funded by any grant.

References

[1] Vaidya, Hanumesh, C. Rajashekhar, K. V. Prasad, Sami Ullah Khan, Arshad Riaz, and J. U. Viharika. "MHD peristaltic flow of nanofluid in a vertical channel with multiple slip features: an application to chyme movement." *Biomechanics and Modeling in Mechanobiology* 20 (2021): 1047-1067. https://doi.org/10.1007/s10237-021-01430-y
[2] Mopuri, Obulesu, A. Sailakumari, Aruna Ganjikunta, E. Sudhakara, K. VenkateswaraRaju, P. Ramesh, Charankumar Ganteda, B. Ramakrishna Reddy, and S. V. K. Varma. "Characteristics of MHD Jeffery Fluid Past an Inclined Vertical Porous Plate." *CFD Letters* 16, no. 6 (2024): 68-89. https://doi.org/10.37934/cfdl.16.6.6889
[3] Nadeem, S., S. Akhtar, and A. Saleem. "Peristaltic flow of a heated Jeffrey fluid inside an elliptic duct: streamline analysis." *Applied Mathematics and Mechanics* 42 (2021): 583-592. https://doi.org/10.1007/s10483-021-2714-6
[4] Gudekote, Manjunatha, and Rajashekhar Choudhari. "Slip effects on peristaltic transport of Casson fluid in an inclined elastic tube with porous walls." *Journal of Advanced Research in Fluid Mechanics and Thermal Sciences* 43, no. 1 (2018): 67-80.
[5] Hamrelaine, Salim, Fateh Mebarek-Oudina, and Mohamed Rafik Sari. "Analysis of MHD Jeffery Hamel flow with suction/injection by homotopy analysis method." *Journal of Advanced Research in Fluid Mechanics and Thermal Sciences* 58, no. 2 (2019): 173-186.
[6] Manjunatha, G., C. Rajashekhar, Hanumesh Vaidya, K. V. Prasad, and K. Vajravelu. "Impact of heat and mass transfer on the peristaltic mechanism of Jeffery fluid in a non-uniform porous channel with variable viscosity and thermal conductivity." *Journal of Thermal Analysis and Calorimetry* 139, no. 2 (2020): 1213-1228. https://doi.org/10.1007/s10973-019-08527-8
[7] Madhukesh, Javali K., Ballajja C. Prasannakumara, Ravikumar S. Varun Kumar, Amar Rauf, and Sabir Ali Shehzad. "Flow of hydromagnetic micropolar-casson nanofluid over porous disks influenced by cattaneo-christov theory and slip effects." *Journal of Porous Media* 25, no. 3 (2022): 35-49. https://doi.org/10.1615/JPorMedia.2021039254
[8] Rajashekhar, C., G. Manjunath, Hanumesh Vaidya, Kerehalli Vinayaka Prasad, B. B. Divya, and J. Saraswati. "Analysis of peristaltic flow of Rabinowitsch fluid in a non-uniform channel: analytical approach." *Latin American Applied Research-An international Journal* 50, no. 3 (2020): 151-158. https://doi.org/10.52292/j.laar.2020.213

[9] Madhukesh, Javali Kotresh, Gosikere Kenchappa Ramesh, Sabir Ali Shehzad, Sharnappa Chapi, and Ingalagondi Prabhu Kushalappa. "Thermal transport of MHD Casson-Maxwell nanofluid between two porous disks with Cattaneo-Christov theory." *Numerical Heat Transfer, Part A: Applications* 85, no. 12 (2024): 2008-2023. https://doi.org/10.1080/10407782.2023.2214322

[10] Bajwa, Sana, Saif Ullah, Amnah S. Al-Johani, Ilyas Khan, and Mulugeta Andualem. "Effects of MHD and porosity on Jeffrey fluid flow with wall transpiration." *Mathematical Problems in Engineering* 2022, no. 1 (2022): 6063143. https://doi.org/10.1155/2022/6063143

[11] Channakote, Mahadev M., Dilipkumar V. Kalse, and Asha S. K. "The consequences of wall properties and slip on the peristaltic motion of Jeffery liquid in a non-uniform tube with heat transfer." *International Journal of Creative Research Thoughts (IJCRT)* 10, no. 2 (2022): 300-310.

[12] Krishna, M. Veera, K. Bharathi, and Ali J. Chamkha. "Hall effects on MHD peristaltic flow of Jeffrey fluid through porous medium in a vertical stratum." *Interfacial Phenomena and Heat Transfer* 6, no. 3 (2018). https://doi.org/10.1615/InterfacPhenomHeatTransfer.2019030215

[13] Ramesh, Gosikere Kenchappa, Pradeep N. Hiremath, Javali Kotresh Madhukesh, and Sabir Ali Shehzad. "EMHD micropolar fluid flowing through a micro-structural slipped surface with heat source/sink and chemical reaction." *ZAMM-Journal of Applied Mathematics and Mechanics/Zeitschrift für Angewandte Mathematik und Mechanik* (2024): e202300628. https://doi.org/10.1002/zamm.202300628

[14] Rani, Y. Sunita, MV Ramana Murthy, G. Vani Sree, and G. Kamala. "Jeffrey Fluid Performance on MHD Convective Flow Past a Semi-Infinite Vertically Inclined Permeable Moving Plate in Presence of Heat and Mass Transfer: a Finite Difference Technique." *International Journal of Dynamics of Fluids* 13, no. 2 (2017): 173-195.

[15] Nallapu, Santhosh, and G. Radhakrishnamacharya. "Jeffrey fluid flow through a narrow tubes in the presence of a magnetic field." *Procedia Engineering* 127 (2015): 185-192. https://doi.org/10.1016/j.proeng.2015.11.325

[16] Kumar, Y. V. Ravi, S. Rajender, S. V. H. N. P. Krishna Kumari, and S. Sreenadh. "Peristaltic pumping of a Jeffrey fluid in an asymmetric channel with permeable walls." *Malaya Journal of Matematik* 2, no. 02 (2014): 141-150. https://doi.org/10.26637/mjm202/006

[17] Kodi, Raghunath, and Obulesu Mopuri. "Unsteady MHD oscillatory Casson fluid flow past an inclined vertical porous plate in the presence of chemical reaction with heat absorption and Soret effects." *Heat Transfer* 51, no. 1 (2022): 733-752. https://doi.org/10.1002/htj.22327

[18] Vijayaragavan, R., M. Ramesh, and S. Karthikeyan. "Heat and mass transfer investigation on MHD Casson fluid flow past an inclined porous plate in the effects of Dufour and chemical reaction." *Journal of Xi'an University of Architecture & Technology* 13, no. 6 (2021): 860-873.

[19] Ahmed, Sameh E., Z. A. S. Raizah, and Ali Chamkha. "Mixed convective transport in inclined porous open arc-shaped enclosures saturated by nanofluids using a second-order Boussinesq approximation." *Case Studies in Thermal Engineering* 27 (2021): 101295. https://doi.org/10.1016/j.csite.2021.101295

[20] Manchi, Ramakrishna, and R. Ponalagusamy. "Modeling of pulsatile EMHD flow of Au-blood in an inclined porous tapered atherosclerotic vessel under periodic body acceleration." *Archive of Applied Mechanics* 91, no. 7 (2021): 3421-3447. https://doi.org/10.1007/s00419-021-01974-6

[21] Sandhya, A., G. V. Ramana Reddy, and V. S. R. G. Deekshitulu. "Heat and mass transfer effects on MHD flow past an inclined porous plate in the presence of chemical reaction." *International Journal of Applied Mechanics and Engineering* 25, no. 3 (2020). https://doi.org/10.2478/ijame-2020-0036

[22] Manjunatha, Gudekote, C. Rajashekhar, Hanumesh Vaidya, and Kerehalli Vinayaka Prasad. "Simultaneous effects of heat transfer and variable viscosity on peristaltic transport of casson fluid flow in an inclined porous tube." *International Journal of Applied Mechanics and Engineering* 24, no. 2 (2019): 309-328. https://doi.org/10.2478/ijame-2019-0020

[23] Krishna, Kumari S. V. H. N. P., D. Saroj Vernekar, and Y. V. K. Ravi Kumar. "A study on the effect of peristalsis and cilia of MHD Micropolar fluid flow through an inclined porous channel." *Journal of Applied Fluid Mechanics* 11, no. 5 (2018): 1321-1331. https://doi.org/10.29252/jafm.11.05.28745

[24] Sharma, Bhupesh Dutt, and Pramod Kumar Yadav. "A two-layer mathematical model of blood flow in porous constricted blood vessels." *Transport in Porous Media* 120 (2017): 239-254. https://doi.org/10.1007/s11242-017-0918-9

[25] Saleem, Anber, Salman Akhtar, Sohail Nadeem, and Mehdi Ghalambaz. "Microphysical analysis for peristaltic flow of SWCNT and MWCNT carbon nanotubes inside a catheterised artery having thrombus: irreversibility effects with entropy." *International Journal of Exergy* 34, no. 3 (2021): 301-314. https://doi.org/10.1504/IJEX.2021.113845

[26] Abuiyada, Alaa, Nabil Eldabe, Mohamed Abouzeid, and Samy Elshaboury. "Influence of both Ohmic dissipation and activation energy on peristaltic transport of Jeffery nanofluid through a porous media." *CFD Letters* 15, no. 6 (2023): 65-85. https://doi.org/10.37934/cfdl.15.6.6585

[27] Saleem, Anber, Salman Akhtar, Sohail Nadeem, Alibek Issakhov, and Mehdi Ghalambaz. "Blood flow through a catheterized artery having a mild stenosis at the wall with a blood clot at the centre." *Computer Modeling in Engineering & Sciences* 125, no. 2 (2020): 565-577. https://doi.org/10.32604/cmes.2020.011883

[28] Akhtar, Salman, L. B. McCash, Sohail Nadeem, and Anber Saleem. "Scientific breakdown for physiological blood flow inside a tube with multi-thrombosis." *Scientific Reports* 11, no. 1 (2021): 6718. https://doi.org/10.1038/s41598-021-86051-2

[29] Misra, Jagadis Chandra, Gopal Chandra Shit, and Ranjan Pramanik. "Non-Newtonian flow of blood in a catheterized bifurcated stenosed artery." *Journal of Bionic Engineering* 15 (2018): 173-184. https://doi.org/10.1007/s42235-017-0014-4

[30] Shahzadi, Iqra, and S. Nadeem. "Role of inclined magnetic field and copper nanoparticles on peristaltic flow of nanofluid through inclined annulus: application of the clot model." *Communications in Theoretical Physics* 67, no. 6 (2017): 704. https://doi.org/10.1088/0253-6102/67/6/704

[31] Reddy, J. V. Ramana, D. Srikanth, and S. V. S. S. N. V. G. Krishna Murthy. "Mathematical modelling of pulsatile flow of blood through catheterized unsymmetric stenosed artery-Effects of tapering angle and slip velocity." *European Journal of Mechanics-B/Fluids* 48 (2014): 236-244. https://doi.org/10.1016/j.euromechflu.2014.07.001

[32] Sharma, Bhupesh Dutt, Pramod Kumar Yadav, and Anatoly Filippov. "A Jeffrey-fluid model of blood flow in tubes with stenosis." *Colloid Journal* 79 (2017): 849-856. https://doi.org/10.1134/S1061933X1706014X